

# Fracture Toughness Analysis of Ceramic and Resin Composite CAD/CAM Material

R Hampe • B Theelke • N Lümke­mann • M Eichberger • B Stawarczyk

## Clinical Relevance

Since breakage is one common reason for restoration failure, the ability to withstand fracture is crucial for the clinical success of dental restorative materials.

## SUMMARY

**Objectives:** To evaluate and compare the fracture toughness of dental CAD/CAM materials of different material classes intended for in-office milling (glass ceramics, hybrid, resin composites) and the influence of aging on this property.

**Methods and Materials:** The fracture toughness (critical intensity factor,  $K_{Ic}$ ) values of 9 CAD/CAM restorative materials (Ambarino High-Class, Brilliant Crios, Cerasmart, exp. CAD/CAM composite, Katana Avencia, Lava

Ultimate, VITA Enamic, IPS Empress CAD, and IPS e.max CAD) were determined using the SEVNB method in a four-point bending setup. Twenty bending bars of each material with a  $4 \times 3$  cross and a minimum length of 12 mm were cut out of CAD/CAM milling blocks. Notching was done starting with a pre-cut and consecutive polishing and v-shaping with a razor blade, resulting in a final depth of v-shaped notches of between 0.8 and 1.2 mm. Half of the specimens were selected for initial fracture toughness measurements. The others were thermocycled in distilled water for  $30,000 \times (5/55^\circ\text{C}; 30\text{-second dwell time})$  before testing. Specimen fracture surfaces were analyzed using confocal laser scanning microscopy.

**Results:** All specimens for each material fractured into two fragments and showed the typical compression curl and brittle failure markings. Comparing initial  $K_{Ic}$  values, lithium disilicate ceramic IPS e.max CAD showed significantly the highest and leucite-reinforced ceramic IPS Empress CAD significantly the lowest  $K_{Ic}$  values ( $p < 0.001$ ). All tested CAD/CAM materials with a resin component ranged in the same  $K_{Ic}$  value group ( $p > 0.999-0.060$ ). After thermal cycling, the highest  $K_{Ic}$  values were measured for lithium disilicate ceramic

\*Rüdiger Hampe, Dipl-Ing (FH), MSc, Department of Prosthetic Dentistry, University Hospital, LMU Munich, Munich, Germany

Björn Theelke, Dipl-Ing (FH), School of Metallurgy and Materials, University of Birmingham, Birmingham, UK

Nina Lümke­mann, MSc, Department of Prosthetic Dentistry, University Hospital, LMU Munich, Munich, Germany

Marlis Eichberger, CDT, Department of Prosthodontics, Dental School Ludwig-Maximilians-University, Munich, Germany

Bogna Stawarczyk, PhD, Dr Dipl-Ing (FH), MSc, Department of Prosthetic Dentistry, University Hospital, LMU Munich, Munich, Germany

\*Corresponding author: Goethestraße 70, Munich, 80336, Germany; e-mail: ruediger.hampe@med.uni-muenchen.de

DOI: <http://doi.org/10.2341/18-161-L>

IPS e.max CAD, followed by resin composite materials Ambarino High-Class ( $p < 0.001-0.006$ ) and hybrid material VITA Enamic ( $p < 0.001-0.016$ ), while the significantly lowest values were reflected for the resin composite materials Cerasmart, LAVA Ultimate ( $p < 0.001-0.006$ ), and Katana Avencia ( $p < 0.001-0.009$ ). The roughness of the fracture surfaces varied depending on the microstructure of the respective material. The ceramic surfaces showed the smoothest surfaces. The fracture surface of VITA Enamic revealed microstructural inhomogeneities and microcracks. For CAD/CAM resin composite materials, crack paths through the matrix and interfaces of matrix and fillers could be observed at the microstructure level.

**Conclusions:** The materials tested show differences in fracture toughness typical for the class they belong to. With one exception (Ambarino High-Class), thermocycling affected the fracture toughness of materials with a resin component negatively, whereas the leucite and lithium disilicate ceramic showed stability.

## INTRODUCTION

Recent technological improvements of CAD/CAM systems with the addition of intraoral camera systems, sophisticated design software, advanced biomaterials, and digital models have led to a significant impact in the area of prosthodontics and restorative dentistry.<sup>1</sup> Traditional processes of restoration fabrication are rated as time consuming, technique sensitive, variable, and unpredictable. CAD/CAM processing with higher standardization offers a good alternative to overcome these issues.<sup>2-4</sup> State-of-the-art restorations can be fabricated using subtractive or additive methods in the dental laboratory or even in the dental office.<sup>1</sup>

In the past, ceramic materials have been used for esthetic restorations manufactured in a manual or CAD/CAM workflow.<sup>5</sup> More recently, resin composites and hybrid materials have been established as an alternative.<sup>3,6</sup> The diversity of restorative materials available for CAD/CAM systems has increased.<sup>7</sup> The polymer-based materials show lower hardness than do ceramic materials, and they can be milled more quickly with less edge chipping and with less wear of milling tools,<sup>8,9</sup> but as a result of the high filler content they behave as brittle materials with linear fracture behavior.<sup>10</sup>

*In situ* restorations are exposed to temperature fluctuation due to breathing, eating, or drinking. In general, temperature changes lead to residual stresses in solid materials. Mechanical properties of materials can be negatively affected and can cause fatigue of the materials.<sup>11,12</sup> Dental resin composite for direct or indirect restorations has shown similar fatigue behavior.<sup>13</sup> In addition, fracture toughness might change as a result of these dynamic temperature changes and other effects of solvents present in the oral environment.<sup>14</sup> In general, polymer networks, such as those present in CAD/CAM resin composite restoratives particularly, tend to be strongly influenced by the wet oral environment.<sup>15</sup> The mechanical behavior of resin composites is unstable under clinical conditions. Therefore, the initial properties do not offer an adequate measurement with which to assess their clinical performance.<sup>16</sup>

Catastrophic breakage by cracking of dental restorations made of brittle materials like resin composite or ceramic is a frequent type of failure.<sup>17-19</sup> Brittle materials show high values for strength, hardness, and Young's modulus, but nevertheless, materials can clinically break at low applied loads. The different failure mechanism of cracking (rather than yielding) shows the need to determine another property with which to characterize the mechanical behavior.<sup>20</sup> Brittle materials are specifically sensitive to defects, which is the reason that they break at lower loads than expected from their strength values. Bearing in mind that void-free objects are practically nonexistent, fracture toughness can be seen as a more relevant property than strength for brittle materials.<sup>21,22</sup> By definition, fracture toughness describes the resistance of a material against the propagation of a preexisting crack.<sup>20</sup> With fracture mechanics methods, the stress distribution in objects with cracks or defects is studied.<sup>23</sup> In contrast to strength values, a significant correlation of clinical fracture and fracture toughness was found for composite resins.<sup>24</sup>

As CAD/CAM resin composite or ceramic restorative materials are brittle by nature they behave in the low-stress regime in an approximately linear elastic manner.<sup>17,25</sup> By introducing a pre-crack or notch, the failure mode "break by cracking" can be induced.<sup>20</sup> Generally, numerous laboratory test methods exist to determine the fracture toughness.<sup>23,26,27</sup> Out of them, the SEVNB method is considered relatively simple compared to other methods with regard to sample preparation.<sup>28</sup> CAD/CAM blocks are limited in size, and bend bars

Table 1: Summary of Selected CAD/CAM Materials Available as Chairside Blocks, Abbreviations, Compositions, Manufacturers, and Lot Numbers

Brand (Lot No.)	Manufacturer	Material Class	Composition <sup>a</sup>
Ambarino High-Class (50712)	Creamed, Marburg, Germany	Resin composite	<ul style="list-style-type: none"> <li>Organic part: Bis-GMA, UDMA, BDMA</li> <li>Inorganic part: 70.1% silicate glass fillers with size of 2-10 <math>\mu\text{m}</math>; average 0.8 <math>\mu\text{m}</math></li> </ul>
Brilliant Crios (H16204)	Coltène/Whaledent, Altstätten, Switzerland	Resin composite	<ul style="list-style-type: none"> <li>Organic part: cross-linked methacrylates</li> <li>Inorganic part: overall 70.7 wt%, barium glass with particle size &lt;1 <math>\mu\text{m}</math> and amorphous silica <math>\text{SiO}_2</math> with particle size &lt;20 nm</li> </ul>
Cerasmart (1407231)	GC, Tokyo, Japan	Resin composite	<ul style="list-style-type: none"> <li>Organic part: UDMA, DMA, Bis-MEPP</li> <li>Inorganic part: 71 wt% barium glass (300 nm), <math>\text{SiO}_2</math> (20 nm)</li> </ul>
exp. CAD/CAM composite (b.28923)	Ivoclar Vivadent, Schaan, Liechtenstein	Resin composite	<ul style="list-style-type: none"> <li>Organic part: resin composite</li> <li>Inorganic part: 80 wt% nanoparticles</li> </ul>
Katana Avencia (115)	Kuraray Noritake Dental, Tokyo, Japan	Resin composite	<ul style="list-style-type: none"> <li>Organic part: UDMA, TEGDMA</li> <li>Inorganic part: 62 wt% aluminum oxide (20 nm), <math>\text{SiO}_2</math> (40 nm)</li> </ul>
Lava Ultimate CAD/CAM Restorative (N525997)	3M, St Paul, MN, USA	Resin composite	<ul style="list-style-type: none"> <li>Organic part: Bis-GMA, Bis-EMA, TEGDMA, UDMA</li> <li>Inorganic part: Silica (20 nm) and zirconia (4-11 nm) fillers and clusters (0.6-10 <math>\mu\text{m}</math>) thereof, filler amount of 79 wt%</li> </ul>
VITA Enamic (43000)	VITA Zahnfabrik, Bad Säckingen, Germany	Hybrid	<ul style="list-style-type: none"> <li>Organic part: UDMA, TEGDMA</li> <li>Inorganic part: glass ceramic (<math>\text{SiO}_2</math>, <math>\text{Al}_2\text{O}_3</math>, <math>\text{Na}_2\text{O}</math>, <math>\text{K}_2\text{O}</math>, <math>\text{B}_2\text{O}_3</math>, <math>\text{ZrO}_2</math>, <math>\text{CaO}</math>) sintered network (86 wt%)</li> </ul>
IPS Empress CAD (T15789)	Ivoclar Vivadent, Schaan, Liechtenstein	Leucite-reinforced glass ceramic	Leucite crystals from 1 to 5 $\mu\text{m}$ embedded in glass matrix; crystal phase: 35-45 vol%
IPS e.max CAD (M26697)		Lithium disilicate glass ceramic	Lithium disilicate crystals ( $\text{Li}_2\text{Si}_2\text{O}_5$ ) embedded in glass matrix; crystal phase: 70 wt%

Abbreviations:  $\text{Al}_2\text{O}_3$ , aluminum oxide;  $\text{B}_2\text{O}_3$ , boron trioxide; BDMA, butanediol dimethacrylate; Bis-EMA, ethoxylated bisphenol-A dimethacrylate; Bis-GMA, bisphenol A glycidylmethacrylate; Bis-MEPP, Bismethacryloxyethoxydiphenylpropane;  $\text{CaO}$ , calcium oxide; DMA, dimethacrylate;  $\text{K}_2\text{O}$ , potassium oxide;  $\text{Na}_2\text{O}$ , sodium oxide;  $\text{SiO}_2$ , silicon dioxide; TEGDMA, triethylenglycol dimethacrylate; UDMA, urethane dimethacrylate;  $\text{ZrO}_2$ , zirconium dioxide.

<sup>a</sup> According to the manufacturer's information.

for testing need to be modified in their dimensions. Here, the SEVNB method is universally applicable, since calculations for  $K_{Ic}$  (critical intensity factor) can be adapted accordingly.<sup>8,23,29</sup> The four-point bending approach is the best discriminating method to use when determining fracture toughness of resin composites with different microstructures.<sup>30</sup>

A retrospective analysis of specimen fracture surfaces helps to investigate the crack propagation process by recognizing typical patterns.<sup>10,23</sup> The aim of the present study was to evaluate and compare the fracture toughness of dental CAD/CAM materials of different material classes intended for in-office milling (glass ceramics, hybrid, resin composites) and the influence of aging on this property. The tested null hypotheses were the following: 1) All materials show comparable  $K_{Ic}$  values, and 2) Aging does not influence the fracture toughness of the tested CAD/CAM materials.

## METHODS AND MATERIALS

Fracture toughness  $K_{Ic}$  values of nine CAD/CAM restorative materials (Ambarino High-Class, Brill-

liant Crios, Cerasmart, exp. CAD/CAM composite, Katana Avencia, Lava Ultimate, VITA Enamic, IPS Empress CAD, and IPS e.max CAD) were determined using the SEVNB method (Table 1). For testing fracture toughness via the SEVNB method, bending bars of  $4 \times 3$  cross-sectional dimension and of a minimum length of 12 mm were cut out of CAD/CAM milling blocks under water cooling with a precision cutting machine (Secotom-50, Struers, Ballerup, Denmark) at 2200 rpm and a feed rate of 0.08 mm/s. IPS e.max CAD specimens required a firing postprocessing step and were crystallized at 840°C according to the manufacturer's instructions (Programat EP 5000, Ivoclar Vivadent, Schaan, Liechtenstein). Crystallization was completed before notch preparation. To create the notch, up to seven specimens of a material were positioned side by side on a specifically designed and customized flat holder. The holder fitted into a precision cutting machine to create the pre-cut and in a razor blade notching machine (SD Mechatronik, Feldkirchen-Westerham, Germany) for final polishing and v-shaping of the ground notch. As lubricant and abrasive medium, a diamond suspension (DiaPro

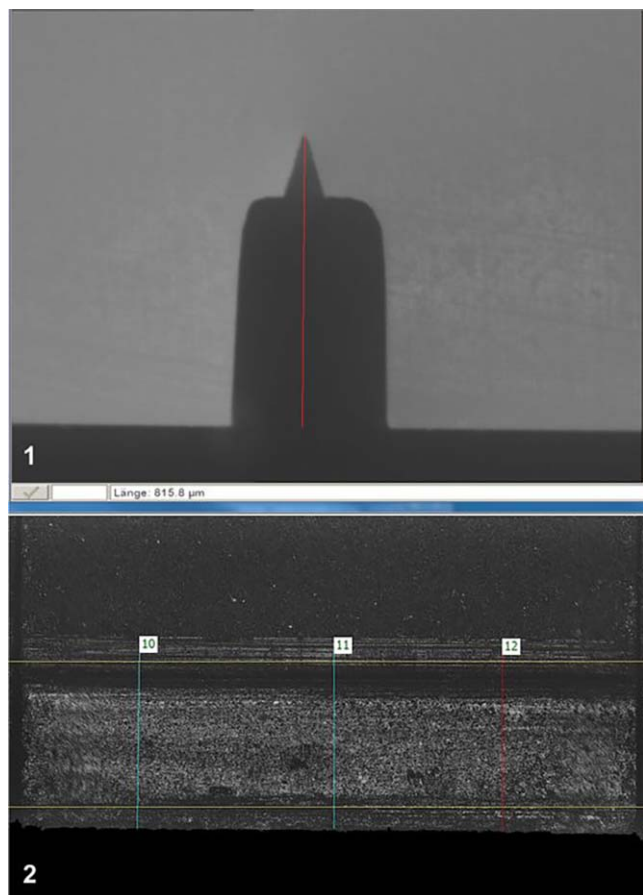


Figure 1. Pre-test depth estimation of specimen (CS) with prepared v-shaped notch.

Figure 2. Determination of notch depth at three locations post testing in order to calculate fracture toughness.

Allegro and DiaPro Dac3; Struers) was used. In accordance with the ISO standard,<sup>28</sup> the final depth of the v-shaped notches was between 0.8 and 1.2 mm. Notch depth was checked (Figure 1) using the microscope of the Martens hardness device with the line measurement function (ZHU 0.2, Zwick Roell, Ulm, Germany).

Twenty specimens with dimensions valid to allow calculations for fracture toughness, as described in ISO 6872, were needed for each material.<sup>28</sup> For safety's sake, more than 20 samples were prepared per material. The 20 specimens needed for the study were arbitrarily selected and randomly distributed to the groups. Half of them were assigned to the thermocycling group (n=10). The others were used for initial fracture toughness measurements (n=10). After preparation of notches, specimens were cleaned with distilled water in an ultrasonic bath (Ultrasonic T-14; L&R Manufac-

turing Co, Kearny, NJ, USA) for five minutes, and all were stored under standard climate conditions (23°C/50% humidity) until testing. For aging, specimens underwent a thermocycling regime of 30,000 cycles in a 5/55°C distilled water bath using Thermocycler THE 1100 (SD Mechatronik, Feldkirchen-Westerham, Germany). All specimens were stored in the same basket. The transition time was set at three seconds and the dwell time at 30 seconds.

Fracture toughness was analyzed according to ISO standard ISO 6872.<sup>28</sup>  $K_{Ic}$  was determined in four-point bending with a crosshead speed of 0.5 mm/min in a universal testing machine (1445 Zwick/Roell, Zwick).

To calculate the mean depth of each notch, the depth was measured post testing at three points on laser scanning microscope images of fracture surfaces after  $K_{Ic}$  testing using the line measurement tool of the image analysis software (VK Analysis module 3.3.0.0; Keyence, Osaka, Japan; see Figure 2). The images were obtained using a microscope (VK-X200; Keyence).

Specimen fracture surfaces were analyzed using confocal laser scanning microscopy. For each specimen tested, one image of the fracture surface was obtained using a microscope (VK-X200; Keyence) with a 20× objective lens, resulting in a 400× digital magnification. In some cases, additional scans with a 50× objective lens, resulting in a 1000× digital magnification, were obtained to assess details of interest on the fracture surfaces. All scans were processed with dedicated image analysis software (VK Analysis module 3.3.0.0; Keyence). The laser scanning microscopy conducted uses a violet laser with a 408 nm wavelength. All scans were done in the high-precision measurement mode. Laser intensity was adapted accordingly to gain optimum quality of scans.

Fracture toughness expressed as critical stress intensity factor ( $K_{Ic}$ ) was calculated for each single specimen tested with the formula given in the ISO standard.<sup>28</sup>

$$K_{Ic} = \frac{F}{b\sqrt{\omega}} \times \frac{S_1 - S_2}{\omega} \times \frac{3\sqrt{\alpha}}{2(1 - \alpha)^{1.5}} \gamma$$

With F (fracture load) in Newtons, b (the bar specimen's width),  $\omega$  (the bar specimen's height), S (the roller span; 1 = outer and 2 = inner), a (notch depth) in millimeters,  $\alpha$  (ratio of notch depth a and specimen's height  $\omega$ ),  $\gamma$  (geometric shape factor),

Table 2: Descriptive Statistics of Fracture Toughness $K_{Ic}$				
Material	Aging	Mean (SD)	95% CI	Min/Median/Max
Ambarino High-Class	Initial	1.43 (0.27)	(1.2;1.7)	1.18/1.38/2.13
	Thermocycling	1.22 (0.33)	(1.0;1.5)	0.93/1.11/2.16
Brilliant Crios	Initial	1.41 (0.14)	(1.3;1.5)	1.25/1.40/1.64
	Thermocycling	1.00 (0.13)	(0.9;1.1)	0.82/1.05/1.15
Cerasmart	Initial	1.22 (0.20)	(1.1;1.4)	0.95/1.21/1.65
	Thermocycling	0.71 (0.07)	(0.6;0.8)	0.59/0.70/0.81
Exp. CAD/CAM composite	Initial	1.37 (0.17)	(1.2;1.5)	1.06/1.33/1.71
	Thermocycling	1.00 (0.17)	(0.8;1.1)	0.77/0.96/1.28
Katana Avencia	Initial	1.47 (0.28)	(1.2;1.7)	1.14/1.45/2.03
	Thermocycling	0.81 (0.16)	(0.7;1.0)	0.61/0.78/1.16
LAVA Ultimate	Initial	1.29 (0.15)	(1.1;1.4)	1.08/1.25/1.62
	Thermocycling	0.74 (0.47)	(0.3;1.2)	0.11/0.69/1.34
VITA Enamic	Initial	1.24 (0.18)	(1.1;1.4)	0.91/1.21/1.57
	Thermocycling	1.09 (0.10)	(1.0;1.2)	0.93/1.09/1.33
IPS Empress CAD	Initial	0.84 (0.48)	(0.5;1.2)	0.13/1.07/1.32
	Thermocycling	1.01 (0.14)	(0.9;1.1)	0.59/1.04/1.16
IPS e.max CAD	Initial	2.15 (0.24)	(2.0;2.3)	1.72/2.21/2.52
	Thermocycling	2.18 (0.22)	(2.0;2.4)	1.69/2.25/2.46
Abbreviations: CI, confidence interval; Max, maximum; Min, minimum; SD, standard deviation.				

which was calculated as follows and in accordance with ISO standard as well.

$$\Upsilon = 1.9887 - 1.326\alpha - \frac{(3.49 - 0.68\alpha + 1.35\alpha^2)\alpha(1 - \alpha)}{(1 + \alpha)^2}$$

Kolmogorov-Smirnov test was used for testing the normal distribution. Univariate analyze of variance with partial eta squared ( $\eta_p^2$ ), Kruskal-Wallis, and Mann-Whitney *U*-test were used to evaluate the data and determine the significant differences between the groups (SPSS Inc, Chicago, IL, USA;  $\alpha=0.05$ ).

RESULTS

The initial mean values of  $K_{Ic}$  and mean values of  $K_{Ic}$  after thermocycling—with their corresponding confidence intervals as well as the minimum, median, and maximum values before and after thermocycling—are summarized in Table 2. For better comparison between materials and the respective effect of thermocycling, the mean values before and after thermocycling are presented side by side in Figure 3.

The Kolmogorov-Smirnov test indicated a higher rate of violation of the normality assumption for  $K_{Ic}$  values (11%), which might be attributed to single statistical outliers. Therefore, the “no assumption of normal distribution” was used for all further statistical tests. The highest impact on  $K_{Ic}$  was exerted by

the CAD/CAM material ( $\eta_p^2=0.720$ ,  $p<0.001$ ), followed by aging level ( $\eta_p^2=0.297$ ,  $p<0.001$ ) and interactions between CAD/CAM material and aging level ( $\eta_p^2=0.253$ ,  $p<0.001$ ).

The univariate analyzed interaction (CAD/CAM material vs aging level) was significant ( $p<0.001$ ). Therefore, the fixed effects of CAD/CAM material and aging level cannot be compared directly, as the higher order interactions were found to be significant. Consequently, several different analyses were computed and divided by levels of CAD/CAM material and aging level depending on the hypothesis of interest.

Impact of CAD/CAM Material on  $K_{Ic}$  Values

Within initially measured groups, IPS e.max CAD showed the significantly highest and IPS Empress CAD the significantly lowest  $K_{Ic}$  values ( $p<0.001$ ). All tested CAD/CAM resin composites as well as VITA Enamic ranged in the same  $K_{Ic}$  values group ( $p>0.999$ -0.060) and were significantly lower compared to IPS e.max CAD and significantly higher compared to IPS Empress CAD ( $p<0.001$ ).

After thermocycling, the highest  $K_{Ic}$  values were measured for IPS e.max CAD ( $p<0.001$ ), followed by Ambarino High-Class ( $p<0.001$ -0.006) and VITA Enamic ( $p<0.001$ -0.016), while the significantly lowest values were displayed for Cerasmart

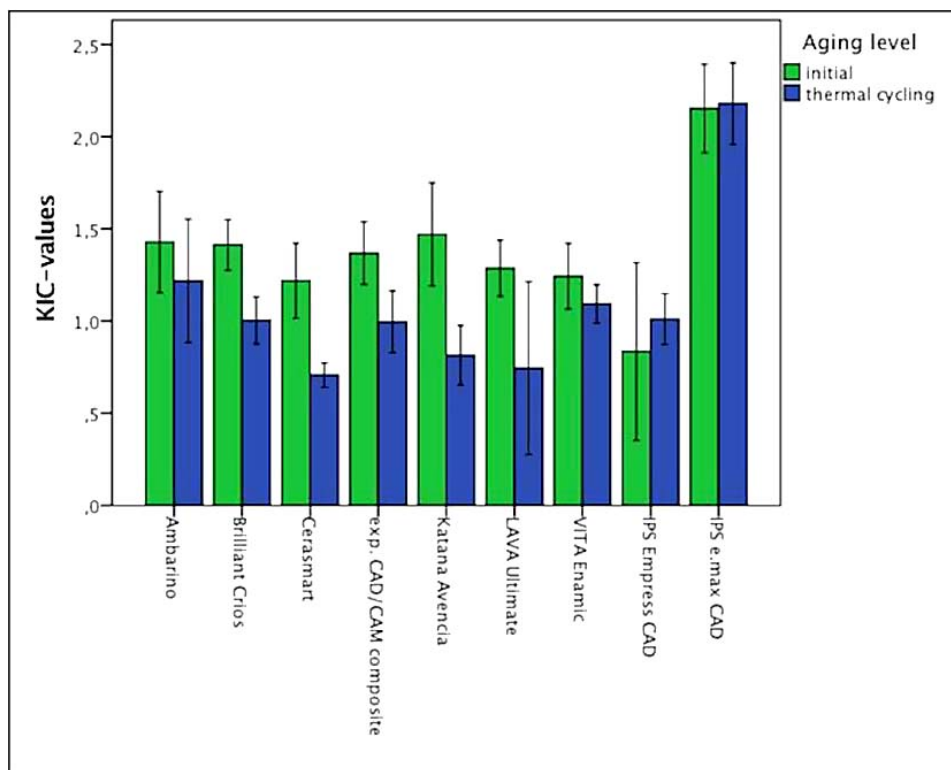


Figure 3.  $K_{IC}$  values initially and after thermal cycling.

( $p < 0.001$ -0.016), LAVA Ultimate ( $p < 0.001$ -0.006), and Katana Avencia ( $p < 0.001$ -0.009).

### Impact of Thermocycling on $K_{IC}$ Values

The  $K_{IC}$  values of the groups Ambarino High-Class ( $p = 0.127$ ), IPS Empress CAD ( $p = 0.247$ ), and IPS e.max CAD ( $p = 0.772$ ) showed no impact of additional thermocycling ( $p = 0.127$ -0.772). The remaining CAD/CAM materials showed a decrease of  $K_{IC}$  values after thermocycling, compared to initial values ( $p < 0.001$ ).

### Fractographic Analysis

All specimens for each material fractured into two fragments and showed a typical compression curl. The absence of crack branching or secondary cracks indicate rather low-energy failures. Macroscopic fracture patterns were similar for all materials, with brittle failure markings.

Figure 4 shows a topographic map of an example specimen giving an overview of the entire fracture surface. Figure 5 shows topographic maps of typical fracture surfaces of the fracture origin line for each material tested at 1000× magnification and a false color map of the same surface. The false colors correspond to the surface heights. Mirror regions

were not detectable on surfaces. Coarse and fine microstructural hackle lines occurred as cracks interacted with the local microstructure of the materials. These microstructural hackle lines always began at the artificially introduced notch line and indicated the crack propagation from there.

Fracture surfaces revealed the different microstructures of the materials tested. The roughness of the fracture surfaces varied depending on the microstructure of the respective material.

The ceramic surfaces (IPS e.max CAD and IPS Empress CAD) showed relatively smooth surfaces indicating crack propagation through the glassy matrix. The fracture surface of VITA Enamic was relatively rough in appearance, with a lot of irregularities and microstructural inhomogeneities. Microcracks were visible as well.

For CAD/CAM resin composite materials, crack paths through the matrix and interfaces of matrix and fillers could be observed at the microstructure level. Microcracks were also detectable. Crack bridging was not directly detectable on the fracture surfaces. Solid particle breaks were not detected for any material, but cut and fractured filler agglomerates at the prepared notches were found for Lava Ultimate and for exp. CAD/CAM composite.



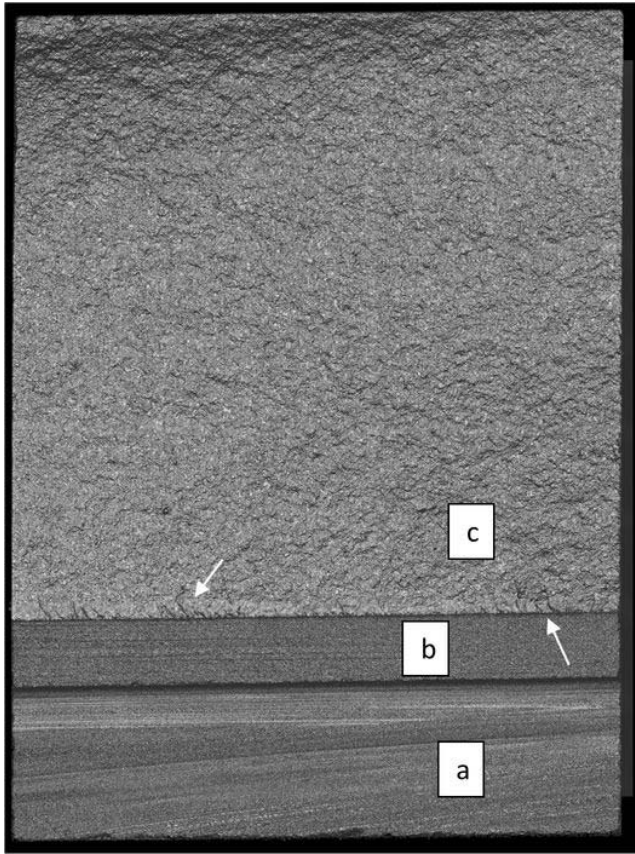


Figure 4. Example of an IPS Empress CAD fracture surface; artificially introduced notch line (border between areas b and c); (a) pre-notch area; (b) polished V-shaped area, a and b with grinding tracks from left to right visible; (c) fracture surface, hackle region with lines away from the notch line, indicating the direction of crack propagation.

## DISCUSSION

The null hypothesis stated that all tested CAD/CAM materials would show comparable  $K_{Ic}$  values, and it is rejected. Initially, the material classes tested showed a statistically significant difference in fracture toughness, which was highest for lithium disilicate ceramic (IPS e.max CAD) and lowest for the leucite-reinforced ceramic (IPS Empress CAD).

As stated in the ADM guidance paper, the literature shows inconsistency in  $K_{Ic}$  values for the same materials, and it is difficult to compare fracture toughness values from different studies.<sup>27</sup> Indentation methods, for example, tend to produce generally greater  $K_{Ic}$  values.<sup>31</sup> Since different methods might lead to different values for the same material, the method with which to determine  $K_{Ic}$  values should always be reported with the values.<sup>23,27</sup> Table 3 gives an overview of recently published fracture toughness values for the materials included in the present study.

For ceramic materials as well as for hybrid material and CAD/CAM resin composites tested, the load-displacement curves indicate linear fracture behavior typical of brittle materials. When tested under static loading, CAD/CAM resin composites show higher or equal failure loads compared to CAD/CAM ceramic restorative materials.<sup>32</sup> However, resin composites are limited by the resin with much lower elastic modulus values.<sup>33</sup> Therefore, the resin composite fracture toughness is governed by the resin matrix.

Values determined for CAD/CAM resin composites with initially  $1.3$  to  $1.5 \text{ MPa} \times \text{m}^{1/2}$  are in the same range as those obtained for direct resin composites.<sup>18</sup> Other studies<sup>24,27,34-36</sup> of fracture toughness of CAD/CAM restorative materials reported a wider range of values (Table 3). Fracture behavior is highly dependent on the microstructure of resin composites.<sup>21</sup> Tortuous fracture surfaces of CAD/CAM resin composites indicate acting toughening mechanisms, but obviously with a limited effect, since the  $K_{Ic}$  values reached are typical for very brittle materials. If the microstructure is not very well controlled and reinforcing particles are not well dispersed or not well connected to the matrix material, the reinforcing particles can act as strength and toughness limiting factors.<sup>10</sup> Whereas the glass ceramics (IPS e.max CAD and IPS Empress CAD) showed no difference in fracture toughness, the hybrid material (VITA Enamic) and all CAD/CAM resin composites, with one exception (Ambarino High-Class), showed a decrease in fracture toughness values. Similar results were reported by Thornton.<sup>37</sup> Because of that, the second null hypothesis that aging does not influence the fracture toughness of CAD/CAM materials needs to be rejected. In general, resin composites are susceptible to fatigue.<sup>38</sup> The chemical stability and solubility of resin composites are especially dependent on organic resin content, silane, and resin composition.<sup>39</sup> The organic resin phase and the silane (filler/matrix interface) have leading roles in the degradation of toughness.<sup>16</sup> Weakening of resin matrix by water facilitates crack propagation.<sup>38</sup> A correlation of filler content level and fracture toughness loss could not be found in this study, which can be interpreted as an indication of a matrix-driven failure mechanism. Sonmez and others<sup>40</sup> also reported a detrimental effect of thermocycling on mechanical properties, especially on materials including an organic phase. The hybrid material VITA Enamic with the polymer-infiltrated glass ceramic network differed significantly from the behavior of glass ceramics (IPS e.max CAD and IPS

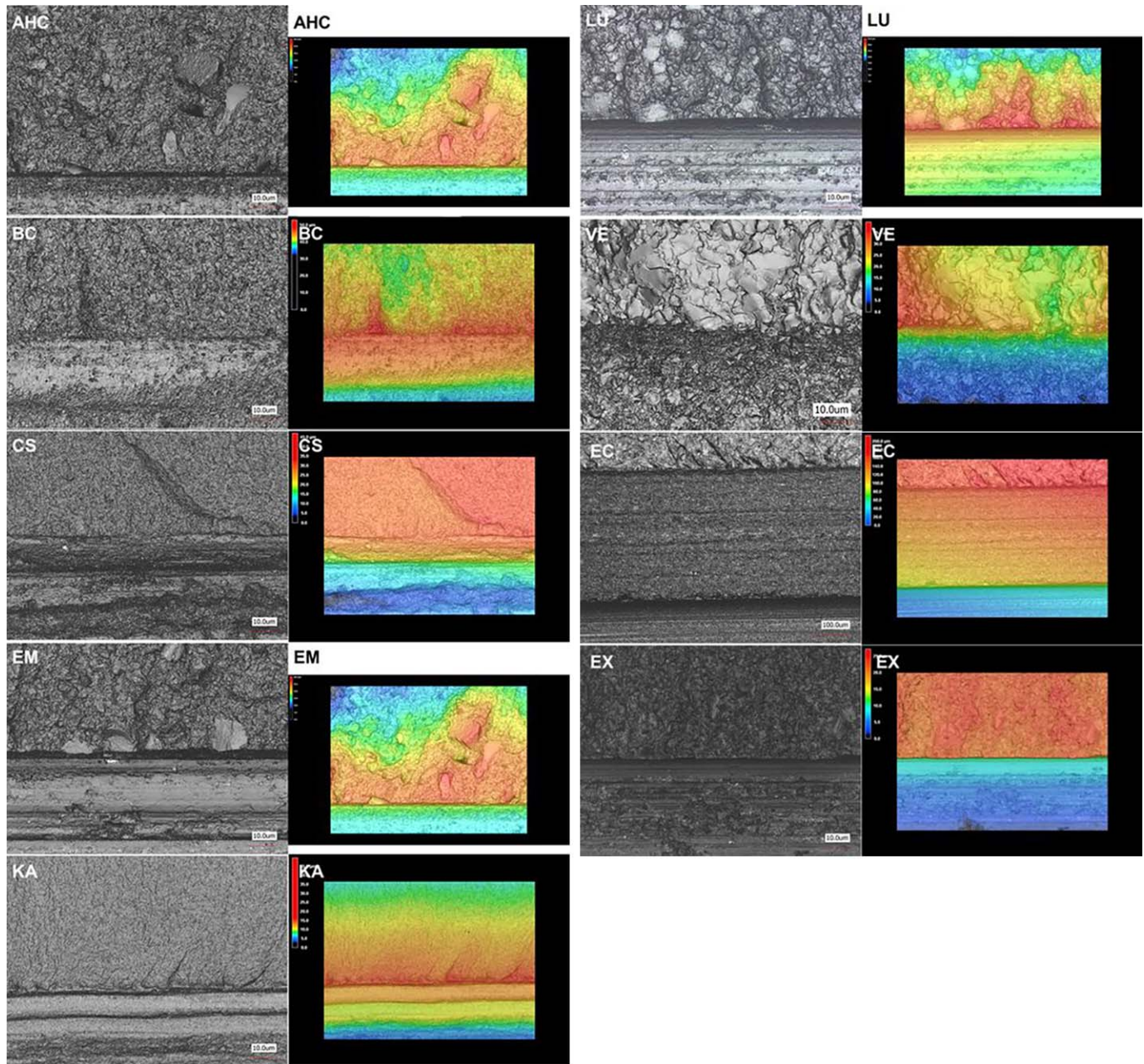


Figure 5. Topographic maps on the left and false color maps of the same region showing the surface height variability. As described in detail in Figure 4 on an IPS Empress CAD fracture surface, fractographic analysis revealed that mirror regions were not detectable on fracture surfaces. Coarse and fine microstructural hackle lines occurred as cracks interacted with the local microstructure of the materials. These microstructural hackle lines always began at the artificially introduced notch line and indicated the crack propagation from there.

Empress CAD) and did not show the same stability against aging. It can be speculated that the thermocycling induced stress at the network interfaces due to differences in the thermal expansion coefficient of the glass ceramic and the polymer parts. This might be the reason why a decrease in fracture toughness was not reported by Ruse and Sadoun<sup>41</sup> when aging was tested for simple water storage for 30 days. The

findings are in accordance with those of Sen and others<sup>42</sup> and Sonmez and others,<sup>40</sup> who also found a decrease of fracture toughness for VITA Enamic after thermocycling. Based on their microstructural analysis, Sonmez and others<sup>40</sup> reported many defects and microcracks after thermocycling.

The macroscopic and microscopic fractographic analyses carried out were qualitative in nature, with



Table 3: *Fracture Toughness Values of CAD/CAM Restorative Materials; If Indicated, "ini" Stands for Initial Values and "TC" for Values Determined After Thermocycling*

Material	$K_{Ic}$ , MPa m <sup>1/2</sup>	Method	Reference
IPS e.max CAD	2 to 2.5	SEVNB	Manufacturer information <sup>a</sup>
	1.8	SEVNB acc. to 6872 in three-point bending setup	34
	1.79	Notchless triangular prism	40
	1.67 (ini); 1.63 (TC)	Vickers Indentation	42
	1.88	Compact Tension	35
IPS Empress CAD	1.90 (ini); 1.88 (TC)	Vickers Indentation	42
VITA Enamic	1.09	SEVNB short beam in three-point setup	29
	1.72	SENB	36
	1.23 (ini); 1.02 (TC)	Vickers Indentation	42
	1.4	SEVNB acc. to 6872 in three-point bending setup	34
	1.0	Compact Tension	35
	0.88 (ini); 0.96 (30 d aged in water)	Notchless triangular prism	40
	1.2	SEVNB acc. to 6872 in three-point bending setup	34
Lava Ultimate	2	SEVNB acc. to 6872 in three-point bending setup	Manufacturer information <sup>b</sup>
	1.6	SEVNB acc. to 6872 in three-point bending setup	34
	1.09	SEVNB short beam in three-point setup	29
	1.29 (ini); 1.10 (TC)	Vickers Indentation	42
	0.8	Compact Tension	35
	0.91 (ini); 0.99 (30 d aged in water)	Notchless triangular prism	40

<sup>a</sup> Obtained from Scientific Documentation IPS e.max CAD.

<sup>b</sup> Obtained from 3M Lava Ultimate CAD/CAM Restorative Technical Product Profile.

the purpose of observing if the specimens fractured as needed for the correct and valid calculation of fracture toughness and to check fracture marks revealing brittle fracture behavior. Furthermore, fractographic analysis revealed different microstructures of the materials and allowed us to identify possible toughening mechanisms. The analysis confirmed that all resin composites are composed of dispersed fillers in a resin matrix. The differences lay in the size, shape, and kind of fillers. The overall irregular tortuous topography of CAD/CAM resin composite fracture surfaces, which was also found by Baudin and others,<sup>21</sup> indicated a toughening mechanism, as evidenced by an increase in the length of the crack path. At the microstructure level, crack deflection at higher strength particles and filler clusters was confirmed as a leading toughening mechanism for all CAD/CAM resin composite materials by observed crack paths through the matrix and along the matrix-filler interfaces. The hybrid VITA Enamic showed another microstructure at the fracture surfaces.

The SEVNB method used in the study can be rated as suitable to measure fracture toughness and to analyze fracture surfaces of dental CAD/CAM restoration materials. In general, defined pre-cracks in small size samples of brittle materials, as required in

this test, are very difficult to control and to realize. Artificial crack-producing methods like the SEVNB method used in this study have become common practice.<sup>19</sup> The small block sizes of chairside CAD/CAM material force researchers to miniaturize bending tests, which makes testing more complex because it requires exact custom fixtures and extra caution in preparation of the specimens. As has been stated before for the SEVNB method,<sup>23</sup> and which this study can confirm, miniaturization is feasible, but differences in specimen preparation were observed. The two tested glass ceramic materials (IPS e.max CAD and IPS Empress CAD) tended toward edge chipping, which is in agreement with the findings of Awada and Nathanson,<sup>8</sup> who tested the edge quality of CAD/CAM materials, including resin composites as well as IPS Empress CAD. The hybrid VITA Enamic was also more prone to chipping and cracking during preparation, compared to the composite resins tested. Here VITA Enamic behaved more typically for a glass ceramic. This observation is in accordance with the edge chipping resistance and toughness results published by Argyrou and others.<sup>43</sup> The tendency of edge chipping of the glass ceramics and the hybrid material can be related to the microstructure and composition. The materials mentioned to be prone to edge chipping have no or

low resin content and show higher surface hardness and indentation modulus.<sup>44</sup> This might contribute to the worse “machinability” of these materials when preparing the specimens.

The SEVNB method is one of the most reportedly reliable methods and has been standardized for dental ceramics in ISO 6872.<sup>28,30</sup> Despite the fact that the method is rated as very reproducible, the published values vary widely. This can be related to intended variations in test setup (eg, three-point or four-point bending) or to difficulties in specimen preparation (eg, producing the v-shaped notch).<sup>27,30</sup> The inherent risk of the method is that the larger tip radii of the artificially introduced notch might lead to overestimation. On the other hand, crack formation during polishing of the v-shaped notch would lead to values that underestimate the true fracture toughness.<sup>23</sup> The notch radius, which can be reached by sharpening, might vary between materials based on their microstructure. The goal is to get a notch radius that is smaller than the major microstructural feature of the material tested in order to measure valid values.<sup>23</sup> The tip radii developed by the method used in this study varied only slightly, and all tip radii were in the range below 20  $\mu\text{m}$ , which is below the recommended maximum limit of 30  $\mu\text{m}$  for resin composites, as stated by Ilie and others,<sup>19</sup> but larger than the fillers used in the resin composite CAD/CAM materials: fine-grain lithium disilicate or leucite crystals of glass ceramics tested in this study (Table 1). This might be a limitation of the SEVNB method in general.

Another limitation of this study is the fact that no *a priori* power analysis was performed to determine sample size. A total of 10 specimens per group were set, considering the results of other studies<sup>35,40</sup> that determined the fracture toughness of dental CAD/CAM restorative materials by working with the same sample sizes as a reference. A pilot study was not performed.

Because of the high depth of field, confocal laser scanning microscopy is predestined for notch depth measurement and for fractography analysis of rough and curved fracture surfaces. It allows not only for high-resolution three-dimensional topographic images but also for roughness and height measurements out of the data, which helps to one to visualize and interpret the fracture patterns.<sup>10</sup> Fractography of dental CAD/CAM materials is challenging. As a result of the inherent microstructural roughness, the fracture surfaces of resin composites, lithium disilicate, and feldspar-based ceramics are difficult to

analyze.<sup>10,45</sup> The microstructure roughness masks the fracture pattern.<sup>10</sup>

Overall, the study setup with the methods used is rated as valid by the authors. To obtain a complete picture of material behavior under clinical conditions, further studies are needed. Thermal changes and moisture are not the only factors causing aging of CAD/CAM restoration materials under clinical conditions.

## CONCLUSIONS

Within the limitations of this *in vitro* study, it can be concluded that

- The fracture toughness of CAD/CAM restorative materials varies widely depending on the material class. Neither the leucite-reinforced ceramic nor the hybrid material nor the resin composites reaches the  $K_{IC}$  level of lithium disilicate ceramic—not even initially.
- Thermocycling affected the fracture toughness of materials with a resin component negatively, whereas the leucite and lithium disilicate ceramic were stable. These differences should be taken into consideration when selecting a restorative material for prosthetic treatments.

## Conflict of Interest

The authors have no proprietary, financial, or other personal interest of any nature or kind in any product, service, and/or company that is presented in this article.

(Accepted 6 November 2018)

## REFERENCES

1. Alghazzawi TF (2016) Advancements in CAD/CAM technology: Options for practical implementation *Journal of Prosthodontic Research* **60**(2) 72-84.
2. Miyazaki T, Nakamura T, Matsumura H, Ban S, & Kobayashi T (2013) Current status of zirconia restoration *Journal of Prosthodontic Research* **57**(4) 208-216.
3. Harada A, Nakamura K, Kanno T, Inagaki R, Örtengren U, Niwano Y, Sasaki K, & Egusa H (2015) Fracture resistance of computer-aided design/computer-aided manufacturing-generated composite resin-based molar crowns *European Journal of Oral Science* **123**(2) 122-129.
4. Miwa A, Kori H, Tsukiyama Y, Kuwatsuru R, Matsushita Y, & Koyano K (2016) Fit of e.max crowns fabricated using conventional and CAD/CAM technology: A comparative study *International Journal of Prosthodontics* **29**(6) 602-607.
5. Fasbinder DJ (2010) Materials for chairside CAD/CAM restorations *Compendium of Continuing Education in Dentistry* **31**(9) 702-709.
6. Mainjot AK, Dupont NM, Oudkerk JC, Dewael TY, & Sadoun MJ (2016) From artisanal to CAD-CAM blocks:

- State of the art of indirect composites *Journal of Dental Research* **95**(5) 487-495.
7. Lambert H, Durand JC, Jacquot B, & Fages M (2017) Dental biomaterials for chairside CAD/CAM: State of the art *Journal of Advanced Prosthodontics* **9**(6) 486-495.
  8. Awada A & Nathanson D (2015) Mechanical properties of resin-ceramic CAD/CAM restorative materials *Journal of Prosthetic Dentistry* **114**(4) 587-593.
  9. Chavali R, Nejat AH, & Lawson NC (2017) Machinability of CAD-CAM materials *Journal of Prosthetic Dentistry* **118**(2) 194-199.
  10. Quinn GD (2016) *Fractography of Ceramics and Glasses* National Institute of Standards and Technology, Washington, DC.
  11. Morresi AL, D'Amarino M, Capogreco M, Gatto R, Marzo G, D'Arcangelo C, & Monaco A (2014) Thermal cycling for restorative materials: Does a standardized protocol exist in laboratory testing? A literature review *Journal of the Mechanical Behavior of Biomedical Materials* **29** 295-308.
  12. Gale MS & Darvell BW (1999) Thermal cycling procedures for laboratory testing of dental restorations *Journal of Dentistry* **27**(7) 89-99.
  13. Belli R, Geinzer E, Muschweck A, Petschelt A, & Lohbauer U (2014) Mechanical fatigue degradation of ceramics versus resin composites for dental restorations *Dental Materials* **30**(4) 424-432.
  14. Shah MB, Ferracane JL, & Kruzic JJ (2009) R-curve behavior and toughening mechanisms of resin based dental composites: Effects of hydration and post-cure heat treatment *Dental Materials* **25**(6) 760-770.
  15. Münchow EA, Ferreira AC, Machado RM, Ramos TS, Rodrigues-Junior SA, & Zanchi CH (2014) Effect of acidic solutions on the surface degradation of a microhybrid composite resin *Brazilian Dental Journal* **25**(4) 321-326.
  16. Lohbauer U, Belli R, & Ferracane JL (2013) Factors involved in mechanical fatigue degradation of dental resin composites *Journal of Dental Research* **92**(7) 584-591.
  17. Nagata K, Garoushi S, Vallittu PK, Wakabayashi N, Takahashi H, & Lassila LVJ (2016) Fracture behavior of single-structure fiber-reinforced composite restorations *Acta Biomaterialia Odontologica Scandinavica* **2**(1) 118-124.
  18. Ilie N, Hickel R, Valceanu AS, & Huth KC (2012) Fracture toughness of dental restorative materials *Clinical Oral Investigation* **16**(2) 489-498.
  19. Ilie N, Hilton TJ, Heintze SD, Hickel R, Watts DC, Silikas N, Stansbury JW, Cadenaro M, & Ferracane JL (2017) Academy of Dental Materials guidance—Resin composites: Part I—Mechanical properties *Dental Materials* **33**(8) 880-894.
  20. Taylor D (2018) Measuring fracture toughness in biological materials *Journal of the Mechanical Behavior of Biomedical Materials* **77** 776-782.
  21. Baudin C, Osorio R, Toledano M, & de Aza S (2009) Work of fracture of a composite resin: Fracture-toughening mechanisms *Journal of Biomedical Materials Research* **89A** 751-758.
  22. Wendler M, Belli R, Petschelt A, Mevec D, Harrer W, Lube T, Danzer R, & Lohbauer U (2017) Chairside CAD/CAM materials. Part 2: Flexural strength testing *Dental Materials* **33**(1) 99-109.
  23. Cesar PF, Bona AD, Scherrer SS, Tholey M, van Noort R, Vichi A, Kelly R, & Lohbauer U (2017) ADM guidance—Ceramics: Fracture toughness testing and method selection *Dental Materials* **33**(6) 575-584.
  24. Heintze SD, Ilie N, Hickel R, Reis A, Loguercio A, & Rousson V (2017) Laboratory mechanical parameters of composite resins and their relation to fractures and wear in clinical trials—A systematic review *Dental Materials* **33**(3) e101-e114.
  25. Shah MB, Ferracane JL, & Kruzic JJ (2009) R-curve behavior and micromechanisms of fracture in resin based dental restorative composites *Journal of the Mechanical Behavior of Biomedical Materials* **2** 502-511.
  26. Zhu X-K & Joyce JA (2012) Review of fracture toughness (G, K, J, CTOD, CTOA) testing and standardization *Engineering Fracture Mechanics* **85** 1-46.
  27. Belli R, Wendler M, Zorzin JI, & Lohbauer U (2018) Practical and theoretical considerations on the fracture toughness testing of dental restorative materials *Dental Materials* **34**(1) 97-119.
  28. ISO-Standards (2015) ISO-6872 Dentistry—Ceramic materials *Geneve: International Organization for Standardization* **11th edition** 1-31.
  29. Della Bona A, Corazza PH, & Zhang Y (2014) Characterization of a polymer-infiltrated ceramic-network material *Dental Materials* **30**(5) 564-569.
  30. Mese A, Palamara JEA, Bagheri R, Fani M, & Burrow MF (2016) Fracture toughness of seven resin composites evaluated by three methods of mode I fracture toughness ( $K_{IC}$ ) *Dental Materials Journal* **35**(6) 893-899.
  31. Sinavart P, Anunmana C, & Muanjit T (2016) Simplified method for determining fracture toughness of two dental ceramics *Dental Materials Journal* **35**(1) 76-81.
  32. Chen C, Trindade FZ, de Jager N, Kleverlaan CJ, & Feilzer AJ (2014) The fracture resistance of a CAD/CAM resin nano ceramic (RNC) and a CAD ceramic at different thicknesses *Dental Materials* **30**(9) 954-962.
  33. Dejak B, Mlotkowski A, & Langot C (2012) Three-dimensional finite element analysis of molars with thin-walled prosthetic crowns made of various materials *Dental Materials* **28**(4) 433-441.
  34. Goujat A, Abouelleil H, Colon P, Jeannin C, Pradelle N, Seux D, & Grosgeat B (2018) Mechanical properties and internal fit of 4 CAD-CAM block materials *Journal of Prosthetic Dentistry* **119**(3) 384-389.
  35. Badawy R, El-Mowafy O, & Tam LE (2016) Fracture toughness of chairside CAD/CAM materials—Alternative loading approach for compact tension test *Dental Materials* **32**(7) 847-852.
  36. He LH & Swain M (2011) A novel polymer infiltrated ceramic dental material *Dental Materials* **27**(6) 527-534.
  37. Thornton I (2014) Mechanical properties of dental resin composite CAD/CAM blocks (T). University of British

- Columbia; Retrieved online January 19, 2018 from: <https://open.library.ubc.ca/cIRcle/collections/24/items/1.0167584>
38. Belli R, Petschelt A, & Lohbauer U (2014) Are linear elastic material properties relevant predictors of the cyclic fatigue resistance of dental resin composites? *Dental Materials* **30**(4) 381-391.
  39. Randolph LD, Palin WM, Leloup G, & Leprince JG (2016) Filler characteristics of modern dental resin composites and their influence on physico-mechanical properties *Dental Materials* **32**(12) 1586-1599.
  40. Sonmez N, Gultekin P, Turp V, Akgungor G, Sen D, & Mijiritsky E (2018) Evaluation of five CAD/CAM materials by microstructural characterization and mechanical tests: A comparative in vitro study *BMC Oral Health* **18**(5) doi.org/10.1186/s12903-017-0458-2
  41. Ruse ND & Sadoun MJ (2014) Resin-composite blocks for dental CAD/CAM applications *Journal of Dental Research* **93**(12) 1232-1234.
  42. Sen D, Sonmez Ceren N, & Turp V (2015) Microstructural characterization and mechanical evaluation of five different CAD/CAM materials *Dental Materials* **31** e2.
  43. Argyrou R, Thompson GA, Cho S-H, & Berzins DW (2016) Edge chipping resistance and flexural strength of polymer infiltrated ceramic network and resin nanoceramic restorative materials *Journal of Prosthetic Dentistry* **116**(3) 397-403.
  44. Hampe R, Lümke mann N, Sener B, & Stawarczyk B (2018) The effect of artificial aging on Martens hardness and indentation modulus of different dental CAD/CAM restorative materials *Journal of the Mechanical Behavior of Biomedical Materials* **86** 191-198.
  45. Scherrer SS, Lohbauer U, Della Bona A, Vichi A, Tholey MJ, Kelly JR, van Noort R, & Cesar PF (2017) ADM guidance—Ceramics: Guidance to the use of fractography in failure analysis of brittle materials *Dental Materials* **33**(6) 599-620.